

# Dual blockade of lipid and cyclin-dependent kinases induces synthetic lethality in malignant glioma

Christine K. Cheng<sup>a,b,c,d</sup>, W. Clay Gustafson<sup>b,d</sup>, Elizabeth Charron<sup>a,b,c,d</sup>, Benjamin T. Houseman<sup>e,f</sup>, Eli Zunder<sup>e,f</sup>, Andrei Goga<sup>d,g</sup>, Nathanael S. Gray<sup>h</sup>, Brian Pollok<sup>i</sup>, Scott A. Oakes<sup>d,j</sup>, C. David James<sup>c,d</sup>, Kevan M. Shokat<sup>d,e,f,k</sup>, William A. Weiss<sup>a,b,c,d,1</sup>, and Qi-Wen Fan<sup>a,b,c,d,1</sup>

Departments of <sup>a</sup>Neurology, <sup>b</sup>Pediatrics, <sup>c</sup>Neurological Surgery and Brain Tumor Research Center, <sup>f</sup>Cellular and Molecular Pharmacology, and <sup>g</sup>Medicine and <sup>h</sup>Helen Diller Family Comprehensive Cancer Center, <sup>e</sup>Program in Chemistry and Chemical Biology, and <sup>i</sup>Department of Cancer Biology, Dana Farber Cancer Institute, Boston, MA 02115; <sup>j</sup>Research and Development, Invitrogen Corp., Carlsbad, CA 92008; and <sup>k</sup>Department of Pathology and <sup>l</sup>Howard Hughes Medical Institute, University of California, San Francisco, CA 94158

Edited by Eric C. Holland, Sloan-Kettering Institute, New York, NY, and accepted by the Editorial Board June 15, 2012 (received for review February 18, 2012)

**Malignant glioma, the most common primary brain tumor, is generally incurable. Although phosphatidylinositol-3-kinase (PI3K) signaling features prominently in glioma, inhibitors generally block proliferation rather than induce apoptosis. Starting with an inhibitor of both lipid and protein kinases that induced prominent apoptosis and that failed early clinical development because of its broad target profile and overall toxicity, we identified protein kinase targets, the blockade of which showed selective synthetic lethality when combined with PI3K inhibitors. Prioritizing protein kinase targets for which there are clinical inhibitors, we demonstrate that cyclin-dependent kinase (CDK)1/2 inhibitors, siRNAs against CDK1/2, and the clinical CDK1/2 inhibitor roscovitine all cooperated with the PI3K inhibitor PIK-90, blocking the antiapoptotic protein Survivin and driving cell death. In addition, overexpression of CDKs partially blocked some of the apoptosis caused by PIK-75. Roscovitine and PIK-90, in combination, were well tolerated in vivo and acted in a synthetic-lethal manner to induce apoptosis in human glioblastoma xenografts. We also tested clinical Akt and CDK inhibitors, demonstrating induction of apoptosis in vitro and providing a preclinical rationale to test this combination therapy in patients.**

Gliomas are the most common primary brain tumors. Glioblastoma multiforme represents the most frequently occurring, highest grade, and most lethal glioma. Amplification of the epidermal growth factor receptor (*EGFR*) occurs in 40% of astrocytomas and correlates with advanced disease (1, 2). *EGFR* signals, in part, through the lipid kinase phosphatidylinositol-3'-kinase (PI3K). Activation of PI3K in glioma also occurs independently of upstream *EGFR*, through gain-of-function mutations in the structural gene for PI3K $\alpha$  (*PIK3CA*) and by loss of phosphatase and tensin homolog (*PTEN*), a lipid phosphatase and negative regulator of PI3K signaling (3).

Given the prominence of signaling through *EGFR* and PI3K in glioma, small-molecule inhibitors of these pathways have tremendous potential as therapeutics. To date, clinical compounds directed against this axis have been tested against *EGFR* and, to a more limited extent, against mammalian target of rapamycin (mTOR), a kinase that signals downstream of PI3K (4). Clinical responses to these agents in glioma have been disappointing, likely, in part, because these therapies are primarily cytostatic rather than apoptotic. In preclinical systems, whereas inhibitors of PI3K effectively block survival signaling by Akt, inhibitors of PI3K alone and in combination with inhibitors of *EGFR* and of the downstream kinase mTOR failed to induce cell death in vitro or in vivo (5, 6).

Our knowledge of the PI3K signaling pathway stems in large part from the development of inhibitors that are either pan-selective or that block specific isoforms within the PI3K family. In screening isoform-selective inhibitors of PI3K, including chemotypes representative of most pharmaceutical drugs entering clinical trials (5, 7), we identified the imidazopyridine

inhibitor, PIK-75, as uniquely able to induce apoptosis rather than growth arrest in glioma. Lacking stability in solution and in vivo (8, 9), the broad target profile and overall toxicity of PIK-75 precluded clinical development. We hypothesized that the efficacy of PIK-75 in inducing apoptosis resulted from a synthetic-lethal interaction between inhibition of PI3K and inhibition of one or more protein kinase targets of PIK-75.

## Results

**PI3K Inhibitor PIK-75 Induces Apoptosis in Glioma.** We screened six glioma cell lines using a panel of PI3K inhibitors including the PI3K $\alpha$ -specific compound PIK-90 (Bayer) and the PI3K/mTOR inhibitors PI-103 (Piramed) and LY294002 (Lilly). In each cell line, flow cytometric analyses demonstrated cell cycle arrest with no appreciable apoptosis (Fig. 1A). In testing additional PI3K inhibitors, we demonstrated that the Piramed p110 $\alpha$ / $\delta$  inhibitor PIK-75 arrested cells and induced apoptosis (Fig. 1A and Fig. S1A). Like PIK-90, PI-103, and LY294002, PIK-75 could block phosphorylation of Akt (Fig. 1B and Fig. S1B). The *PTEN* wild type (WT) cell line LN229 showed increased levels of apoptosis in comparison with the *PTEN* mutant (MT) line U87, using doses of PIK-75 that led to equivalent reductions in p-Akt (Fig. 1C and Fig. S1A and B). In comparing biochemical activity of LY294002 with PIK-75, LY294002 more potently blocked both p-Akt and the mTOR target p-rpS6 (Fig. S1B), and yet LY294002, in contrast to PIK-75, was unable to promote apoptosis.

**Apoptosis Induced by PIK-75 Requires Inhibition of PI3K and Is Mitochondrial-Dependent.** Data in Fig. 1A and B demonstrated that PIK-75 was unique among PI3K inhibitors in inducing apoptosis, suggesting an off-target effect. In contrast, however, data in Fig. 1C demonstrated that the degree of apoptosis induced in response to PIK-75 varied as a function of *PTEN* status, suggesting that apoptosis induced by PIK-75 resulted, at least in part, from PI3K inhibition.

To clarify this issue, we treated LN229 *PTEN*<sup>WT</sup> cells with the *PTEN* inhibitor bisperoxovanadium (bpv) (10). Addition of bpv led to increased levels of p-Akt (Fig. 2A and B) and partially attenuated cell death induced by PIK-75 (Fig. 2C), without affecting induction of G<sub>2</sub>M arrest. This result was also validated in

Author contributions: C.K.C., B.T.H., E.Z., N.S.G., S.A.O., C.D.J., K.M.S., W.A.W., and Q.-W.F. designed research; C.K.C. and Q.-W.F. performed research; W.C.G., E.C., B.T.H., E.Z., A.G., N.S.G., B.P., S.A.O., and C.D.J. contributed new reagents/analytic tools; C.K.C., B.T.H., E.Z., A.G., N.S.G., K.M.S., W.A.W., and Q.-W.F. analyzed data; and C.K.C., W.A.W., and Q.-W.F. wrote the paper.

The authors declare no conflict of interest.

This article is a PNAS Direct Submission. E.C.H. is a guest editor invited by the Editorial Board.

<sup>1</sup>To whom correspondence may be addressed. E-mail: waweiss@gmail.com or qiwen.fan@ucsf.edu.

This article contains supporting information online at [www.pnas.org/lookup/suppl/doi:10.1073/pnas.1202492109/-DCSupplemental](http://www.pnas.org/lookup/suppl/doi:10.1073/pnas.1202492109/-DCSupplemental).

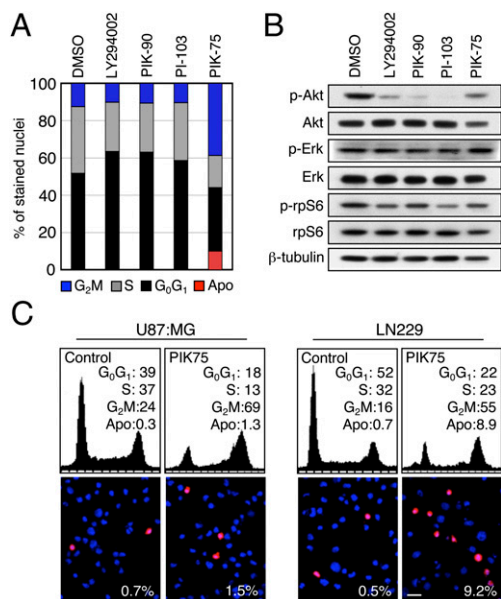


**Fig. 1.** The PI3K inhibitor PIK-75 induces apoptosis and G<sub>2</sub>M arrest in *PTEN*<sup>WT</sup> and *PTEN*<sup>MT</sup> glioma cell lines. (A) *PTEN*<sup>WT</sup> cell line LN229 was treated with DMSO, LY294002 (10 μM), PIK-90 (0.5 μM), PI-103 (0.5 μM), or PIK-75 (0.5 μM) for 24 h. Cells were stained with propidium iodide and analyzed by flow cytometry. In comparison with PIK-90 and PI-103, PIK-75 induced arrest at G<sub>2</sub>M and apoptosis (increase in sub-G<sub>1</sub> fraction). (B) LN229 cells were treated for 6 h with agents and doses used in A and analyzed by immunoblot. All inhibitors blocked p-Akt. (C) Glioma cells mutant (U87) or wild-type (LN229) for *PTEN* were treated with PIK75 (0.5 μM) for 24 h and analyzed by flow cytometry. Cytospins were also analyzed for apoptosis indicated by cleaved caspase 3. (Blue nuclear stain is DAPI.) PIK-75 induced apoptosis most efficiently in cells wild type for *PTEN*.  $P < 0.005$  for U87/PIK-75 and  $P < 0.0001$  for LN229/PIK-75 versus their respective controls.

*PTEN*<sup>WT</sup> LN229 cells stably transduced with Akt-ER (11). Upon addition of the estrogen receptor (ER) agonist 4-hydroxytamoxifen (4-HT), Akt-ER protein was phosphorylated and activated (Fig. S2A). Apoptosis in response to PIK-75 was largely attenuated, whereas G<sub>2</sub>M arrest remained unchanged (Fig. S2B). In addition, an Akt1/2 inhibitor, which alone did not induce apoptosis, was able to override the effects of increased PI3K signaling in U87 *PTEN*<sup>MT</sup> cells, restoring apoptosis in response to PIK-75 (Fig. S2C). Collectively, these experiments demonstrate that apoptosis (but not arrest at G<sub>2</sub>M) required blockade of the PI3K pathway.

To further characterize apoptosis induced by PIK-75, we examined mouse embryonic fibroblasts (MEFs) deficient in the apoptotic effector Bax (12). Wild-type (WT) MEFs were sensitive to apoptosis induced by PIK-75, whereas *BAX*<sup>-/-</sup> MEFs were resistant (Fig. S3A and B). In LN229 glioma cells, knocking down Bax with siRNA also increased resistance to PIK-75 (Fig. 2D and E). Because Bax regulates cell death exclusively through the mitochondrial apoptotic pathway (12, 13), and loss of Bax blocks cell death induced by PIK75, we conclude that apoptosis initiated by PIK-75 proceeds through a mitochondrial-dependent pathway that requires Bax.

**Inhibition of Cyclin-Dependent Kinases and PI3K Induces Synthetic Lethality in Glioma.** PIK-75 was unique among a group of lipid kinase inhibitors screened previously in its ability to block both lipid and serine–threonine kinases (7). We, therefore, reasoned that inhibition of PI3K in combination with inhibition of one or more serine–threonine kinases might uncover a synthetic-lethal combination of lipid and protein kinases, the inhibition of which results in apoptosis. Using SelectScreen Profiling (Invitrogen),

we identified 21 kinases that were inhibited over 95% in response to PIK-75 (Table S1).

From this list of serine–threonine kinases, we tested the cyclin-dependent kinases 1 and 2 (CDK1 and CDK2) because these were strongly inhibited by PIK-75, had well-described roles in regulating the G<sub>2</sub>M transition, and inhibitors of these kinases are now in clinical trials (14, 15). Because G<sub>2</sub> arrest was unique to PIK-75, blockade of CDK1 and/or CDK2 could conceivably contribute to the abilities of PIK-75 to induce apoptosis over other G<sub>1</sub>-arresting PI3K inhibitors. PIK-75 also induced p-Erk (Fig. 1B and Fig. S4A and B). We, therefore, asked whether combination therapy using inhibitors of PI3Kα with inhibitors of CDK1 and/or CDK2 could induce apoptosis, with accompanying biomarkers demonstrating G<sub>2</sub> arrest and induction of p-Erk.

We treated LN229 *PTEN*<sup>WT</sup> cells with small-molecule inhibitors of CDK1 [3-(2-chloro-3-indolylmethylene)-1,3-dihydroindol-2-one] or CDK2 [4-(6-cyclohexylmethoxy-9H-purin-2-ylamino)-*N,N*-diethylbenzamide]. Flow cytometric analysis at 24 h showed that both inhibitors induced arrest at G<sub>2</sub>M (Fig. 3A), and the CDK2 inhibitor demonstrated a dose-dependent increase in p-Erk by immunoblot (Fig. 3B). Combining the CDK1 inhibitor with the PI3Kα inhibitor PIK-90 did not result in appreciable apoptosis (Fig. 3C). Combining the CDK2 inhibitor with PIK-90 did demonstrate an increase in apoptosis in comparison with monotherapy. Levels of apoptosis in response to combination therapy were much lower than those observed using PIK-75 (Fig. 3D) and were limited to LN229 *PTEN*<sup>WT</sup>, with no significant apoptosis seen in *PTEN*<sup>MT</sup> cell lines U87 and U373 (Fig. S1C and D) over monotherapy. These data suggest that blockade of CDK2 cooperates with inhibition of PI3K to drive apoptosis, whereas blockade of CDK1 does not.

To achieve higher selectivity, and to assess whether blockade of CDK1 could further enhance apoptosis observed in response to dual blockade of CDK2 and PI3Kα, we combined siRNAs against CDK1 and CDK2 with small-molecule inhibition of PI3K. Whereas combining PIK-90 with siRNA against CDK1 or CDK2 did not induce appreciable cell death, combining PIK-90 with siRNA against both CDK1 and CDK2 clearly induced apoptosis (Fig. 3E). These data suggest that CDK1, CDK2, and PI3K cooperate to induce therapeutic resistance in glioma and that combined blockade of these three targets, in part, underlies the ability of PIK-75 to induce apoptosis.

To further clarify the relative contribution of CDK1 versus CDK2 in the synthetic-lethal relationship, LN229 cells were stably transduced with retroviral vectors expressing CDK1, CDK2, or both and treated with PIK-75. Apoptosis was assessed by PARP (poly ADP-ribose polymerase) cleavage and annexin V flow cytometry. Whereas apoptosis induced by PIK-75 was affected modestly by overexpression of CDK1, apoptosis was clearly reduced in cells overexpressing CDK2 and attenuated further in response to overexpression of both CDK1 and CDK2 (Fig. 3F and Fig. S5). We conclude that overexpression of these CDKs drives resistance to PIK-75 and that CDK2 overexpression more potently rescues cells from PIK-75-induced cell death compared with CDK1. Collectively, these data support the importance of CDKs as proapoptotic targets of PIK-75.

**Inhibitors of CDK1/2 Cooperate with an Inhibitor of PI3K to Down-Regulate Survivin, Resulting in Apoptosis.** Roscovitine, a kinase inhibitor with potent activity against CDK1 and CDK2, is currently in trials for treatment of solid tumors (16–18). Like PIK-75, roscovitine induced p-Erk (Fig. S4C). We treated LN229 glioma cells with roscovitine alone and in combination with PIK-90. Combination treatment induced apoptosis, as demonstrated by flow cytometric analysis of sub-G<sub>1</sub> fraction and by immunoblot for cleaved PARP (Fig. 4A and B). We validated this result in *PTEN* WT GBM43 cells cultured from a primary glioma xenograft (19). Again, incubation of GBM43

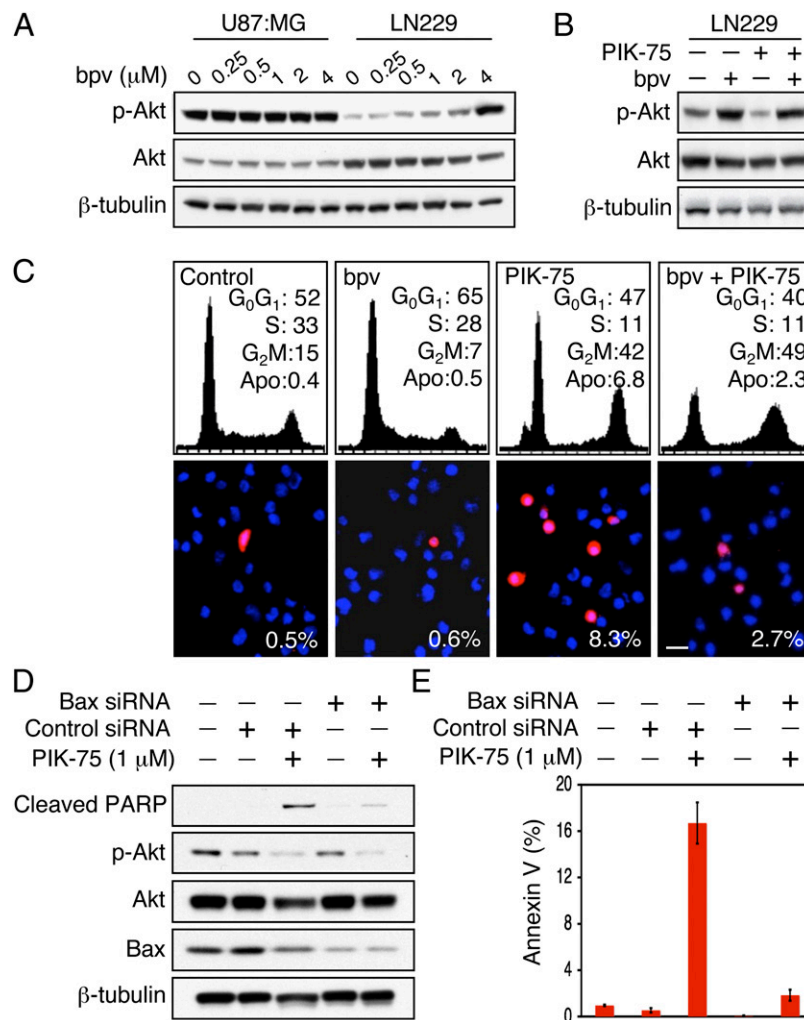


**Fig. 2.** Apoptosis induced by PIK-75 is dependent on inhibition of PI3K and proceeds via a mitochondrial-dependent pathway. (A) U87 and LN229 cells were treated with increasing concentrations of the PTEN inhibitor bpv for 24 h. Blockade of PTEN was monitored by immunoblot, demonstrating increased levels of p-Akt. (B) PIK-75-mediated inhibition of p-Akt was abrogated by bpv. Cells were treated with PIK-75 (0.5 μM) or bpv (3 μM) for 24 h and analyzed by flow cytometry. Cytospins were also analyzed for apoptosis indicated by cleaved caspase 3. (Blue nuclear stain is DAPI.) PIK-75 induced apoptosis and arrest at G<sub>2</sub>M. Addition of bpv abrogated apoptosis without affecting arrest. (C) LN229 cells were treated with PIK75 (0.5 μM), bpv (3 μM), or both for 24 h and analyzed by flow cytometry. Cytospins were also analyzed for apoptosis indicated by cleaved caspase 3. (Blue nuclear stain is DAPI.) PIK-75 induced apoptosis and arrest at G<sub>2</sub>M. Addition of bpv abrogated apoptosis without affecting arrest. (D) LN229 cells were transfected with siRNA against Bax for 24 h and then treated with PIK-75 (1 μM) for 24 h and lysed. Immunoblot analysis shows that knockout of Bax decreased PARP cleavage in the presence of PIK-75, compared with cells with Bax levels in tact. (E) Cells treated as in D were analyzed by flow cytometry for annexin V-FITC. Upon treatment with PIK-75, Bax siRNA-transfected cells showed decreased levels of apoptosis compared with cells transfected with a nontargeting control siRNA.  $P < 0.005$ .

cells with PIK-90 and roscovitine yielded higher levels of apoptosis than either agent alone (Fig. 4C).

In contrast, combination therapy using roscovitine and PIK-90 in *PTEN*<sup>MT</sup> GBM14 primary cells (Fig. 4D) and *PTEN*<sup>MT</sup> glioma cell lines U87 and U373 (Fig. S6) showed a trend toward increased apoptosis, but was not statistically significant, compared with monotherapy. When *PTEN*<sup>WT</sup> breast cancer lines MDAMB231 and T47D and *PTEN*<sup>MT</sup> breast cancer lines BT549 and SUM149 were treated with roscovitine and PIK-90, all but the T47D line showed significant increases in apoptosis with combination therapy over PIK-90 monotherapy, albeit not over roscovitine monotherapy (Fig. S6). Collectively, these data suggest the synthetic-lethal effect of PI3K and CDK inhibition is limited to *PTEN*<sup>MT</sup> glioma cells.

Roscovitine has been shown to reduce levels of the anti-apoptotic protein Survivin (20). To gain insight into mechanism, we investigated levels of Survivin protein in response to roscovitine and PIK-90. siRNA knockdown of Survivin induced apoptosis in LN229 glioma cells (Fig. 4E). Roscovitine treatment,

both alone and in combination with PIK-90, led to reduced levels of Survivin by immunoblot (Fig. 4F). Overexpressing Survivin in LN229 cells rescued them from the apoptotic effects of combination therapy (Fig. 4F), suggesting that inhibitors of PI3K and CDK1/2 induce apoptosis in glioma because of a synthetic-lethal interaction leading to blockade of Survivin.

#### Clinical CDK1/2 Inhibitor Cooperates with PIK-90, Inducing Cell Death in Glioma Xenografts.

To test the efficacy of roscovitine and PIK-90 in vivo, we implanted GBM43 cells s.c. into nude mice. Mice with established tumors were randomized into four treatment groups: vehicle (PBS:H<sub>2</sub>O), roscovitine, PIK-90, or PIK-90 plus roscovitine. After 12 d of treatment, both roscovitine and PIK-90 showed clear single-agent efficacy, with tumor size in mice treated with roscovitine and PIK-90 in combination significantly smaller than either vehicle or monotherapy-treated controls (Fig. 5A). Roscovitine was less effective than PIK-90 in blocking proliferation (levels of Ki-67), whereas combination therapy showed essentially additive antiproliferative effects

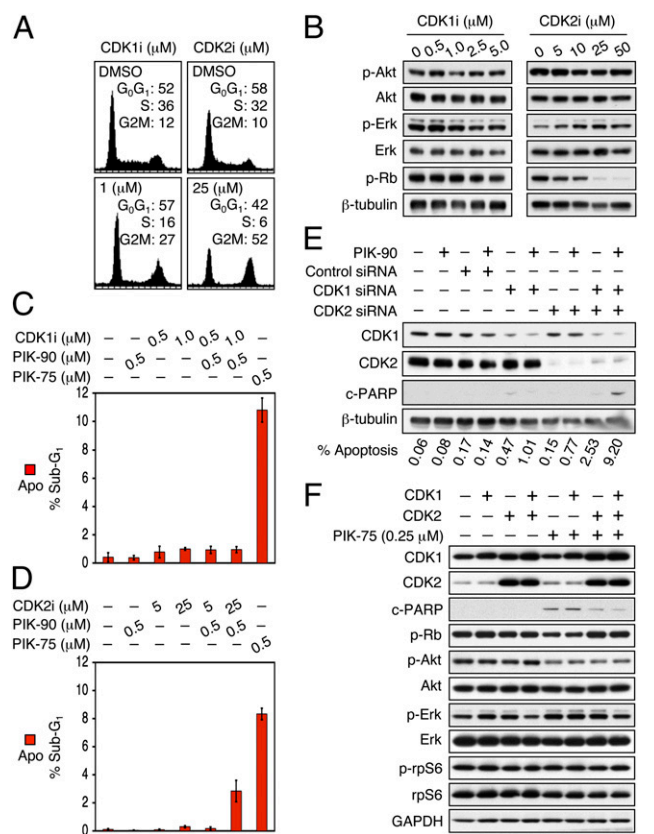


**Fig. 3.** A synthetic-lethal interaction among CDKs and PI3Ks: induction of apoptosis. (A) LN229 cells were treated for 24 h with indicated concentrations of [3-(2-chloro-3-indolylmethylene)-1,3-dihydroindol-2-one], an inhibitor of CDK1, or [4-(6-cyclohexylmethoxy-9H-purin-2-ylamino)-N,N-diethylbenzamide], an inhibitor of CDK2. Both agents induced arrest at G<sub>2</sub>M. (B) LN229 cells were treated with increasing concentrations of CDK1 and CDK2 inhibitors for 24 h and then analyzed by immunoblot. The CDK2 inhibitor induced activation of p-Erk, comparable with results observed using PIK-75 (Fig. S4). (C) LN229 cells were treated for 24 h with indicated concentrations of CDK1 inhibitor, PIK-75, PIK-90, or the combinations shown. The levels of apoptosis (sub-G<sub>1</sub> fraction) achieved by combining CDK1 inhibitor with PIK-90 were much less than those observed with PIK-75 ( $P < 0.05$  for CDK1/PIK-90 combination therapy versus PIK-90 monotherapy;  $P < 0.0001$  for PIK-75 versus DMSO control). (D) LN229 cells were treated for 24 h with indicated concentrations of CDK2 inhibitor, PIK-75, PIK-90, or the combinations shown. The levels of apoptosis (sub-G<sub>1</sub> fraction) achieved by combining CDK2 inhibitor (25 μM) and PIK-90 [ $P < 0.05$  versus CDK2 (25 μM) or PIK-90 monotherapy] were modest compared with PIK-75. (E) LN229 cells were transfected with siRNA against CDK1 and/or CDK2 for 24 h, treated with PIK-90 (0.5 μM) for 72 h, and lysed. Combination therapy using CDK1 and CDK2 siRNAs and PIK-90 led to apoptotic PARP cleavage. Apoptosis (sub-G<sub>1</sub> fraction) was also quantified by flow cytometry, showing the highest levels for combination therapy using both CDK siRNAs and PIK-90. (F) LN229 cells stably transduced with CDK1 and/or CDK2 were treated with PIK-75 (0.25 μM) for 24 h and lysed. PIK-75 induced PARP cleavage in both parental and CDK1-overexpressing cells. PARP cleavage was decreased in CDK2-overexpressing cells and further decreased in cells that overexpressed both CDK1/2.

(Fig. 5B). Neither agent as monotherapy induced appreciable apoptosis (cleaved caspase 3).

Because GBM43 is fast-growing, tumors in the control group reached intolerable sizes and, at the time of sacrifice, necessitated by size of control tumors and required by our Institutional Animal Care and Use Committee (IACUC) protocol, no clear regression was observed. Nevertheless, roscovitine and PIK-90 led to combinatorial efficacy in driving apoptosis in vivo, with 7.8% of tumor cells staining positively for cleaved caspase 3, compared with 0.6% for tumors treated with roscovitine single

agent and 1.6% for tumors treated with PIK-90 as monotherapy. The treatments were well tolerated, with no overt signs of toxicity measured during the trial or at necropsy. Collectively, these experiments suggest that combined inhibition of PI3K, CDK1, and CDK2 can convert a cytostatic therapy into an apoptotic one in malignant glioma, offering a therapeutic rationale translatable to patients with glioma.

MK-2206 is an orally active allosteric Akt inhibitor in clinical trials (21). MK-7965 is an inhibitor of CDK1 and -2 (as well as

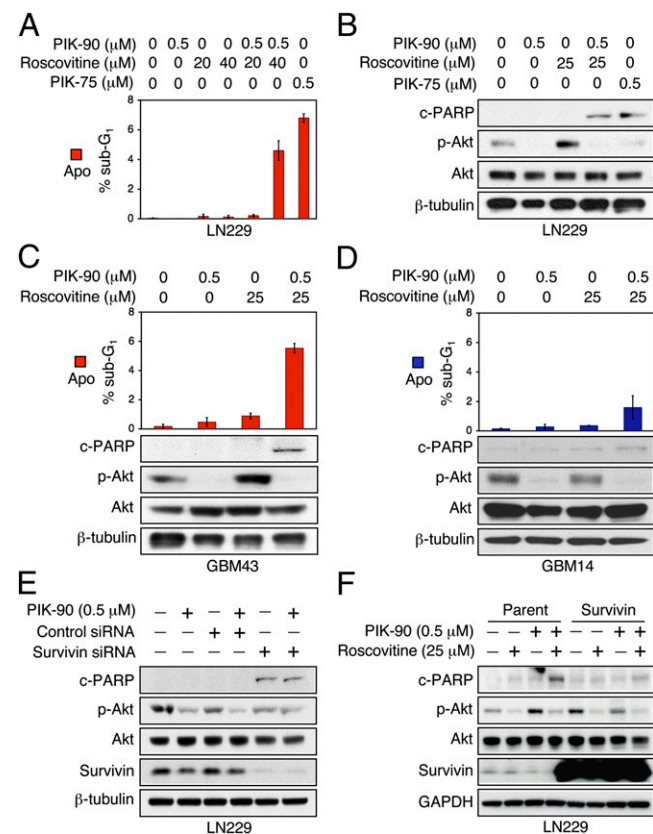


**Fig. 4.** Combination therapy with roscovitine and PIK-90 induces apoptosis in glioma cells. (A) LN229 cells were treated with indicated concentrations of roscovitine and 0.5 μM PIK-90 for 24 h. Combination therapy using roscovitine with PIK-90 induced significant levels of apoptosis (sub-G<sub>1</sub> fraction) at 40 μM roscovitine ( $P < 0.01$  for combination therapy versus PIK-90 or roscovitine monotherapy). (B) LN229 cells were treated with 25 μM roscovitine, 0.5 μM PIK-90, and 0.5 μM PIK-75 for 6 h and then lysed and analyzed by immunoblot. Both PIK-90 and PIK-75 inhibited p-Akt. Combination therapy using roscovitine with PIK-90 induced cleavage of PARP comparable with levels observed in PIK-75-treated cells. (C) GBM43 *PTEN*<sup>WT</sup> primary glioma cells were treated with 25 μM roscovitine and 0.5 μM PIK-90 for 24 h. Combination therapy with roscovitine and PIK-90 induced significant levels of apoptosis (sub-G<sub>1</sub> fraction) ( $P < 0.0001$  versus PIK-90 or roscovitine monotherapy). Cell lysates were analyzed by immunoblot, showing induction of PARP cleavage by combination therapy. (D) GBM14 *PTEN*<sup>MT</sup> primary glioma cells were treated with 25 μM roscovitine and 0.5 μM PIK-90 for 24 h. Combination therapy with roscovitine and PIK-90 induced insignificant levels of apoptosis (sub-G<sub>1</sub> fraction). Cell lysates were analyzed by immunoblot, showing less induction of PARP cleavage compared with C. (E) LN229 cells were transfected with siRNA against Survivin (24 h) and then treated with PIK-90 (0.5 μM; 48h) and lysed. The immunoblot shows levels of Survivin protein. Both Survivin siRNA alone and in combination with PIK-90 led to cleavage of PARP. (F) LN229 cells, WT and Survivin-overexpressing, were treated with 25 μM roscovitine and 0.5 μM PIK-90 for 6 h and then lysed and analyzed by immunoblot. Roscovitine decreased Survivin levels in the WT cells, and combination therapy with roscovitine and PIK-90 induced cleavage of PARP in the WT but not Survivin-overexpressing cells.

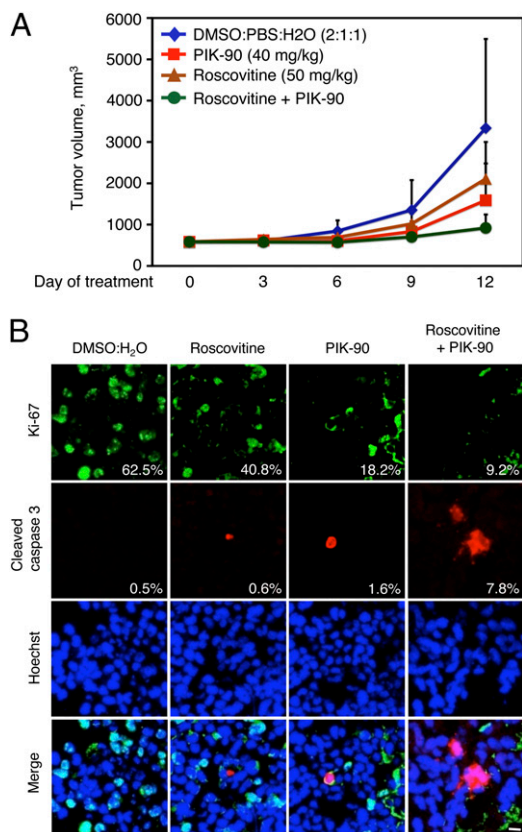


**Fig. 5.** Combination therapy with roscovitine and PIK-90 induces apoptosis in vivo: a clinically translatable synthetic-lethal interaction. (A) Mice with established tumors were treated by daily i.p. injection of PIK-90 (40 mg/kg) and roscovitine (50 mg/kg). The graph shows mean tumor volume  $\pm$  SE obtained from three (control) or four mice (all other groups). Roscovitine and PIK-90 showed combinatorial efficacy in reducing tumor volume over monotherapy ( $P < 0.05$  for combination therapy versus roscovitine monotherapy). (B) Immunohistochemical analysis was performed on residual tumors killed on day 12 of therapy. Roscovitine and PIK-90 showed combinatorial efficacy in driving apoptosis in vivo, with 7.8% of cells staining positively for cleaved caspase 3 in tumors treated with combination therapy, compared with 0.6% for tumors treated with roscovitine single agent ( $P < 0.0001$ ) and 1.6% for tumors treated with PIK-90 as monotherapy ( $P < 0.0001$ ).

CDK5 and -9) that is also under clinical evaluation (22). In LN229 glioma cells, MK-2206 effectively inhibited Akt (Fig. S7A). MK-7965 led to decreases in p-Rb and increases in p-Erk levels (Fig. S7B). Combination therapy resulted in increased apoptosis compared with either monotherapy arm (Fig. S7C and D). These data show that inhibiting the PI3K pathway at the level of Akt in combination with this CDK inhibitor would also lead to synthetic lethality in glioma and offers a combination of agents readily translatable to patients.

## Discussion

If successful cancer therapies need to target multiple kinases, is it reasonable to discard polyspecific compounds that fail preclinically or clinically because of toxicity? Among such compounds, if one can distinguish targets required for synthetic-lethal interactions specific to tumor cells, from those that contribute non-specifically to toxicity, can new compounds or combinations be identified that retain efficacy in the setting of an improved toxicity profile? In screening a broad range of PI3K inhibitors, including chemotypes representative of most drugs currently in clinical development, we identified PIK-75 as an inhibitor of PI3K $\alpha$  that potently induced apoptosis in glioma. However,

because of both toxicity and poor drug-like properties, PIK-75 was unsuitable for clinical use in cancer therapy.

Using the concept that increased selectivity should correlate with decreased toxicity, we reasoned that inhibition of a select group of PIK-75 targets in combination with inhibition of PI3K might represent a synthetic-lethal approach, inducing apoptosis while retaining a tolerable toxicity profile. We first demonstrated that inhibition of PI3K contributed to apoptosis induced by PIK-75. Next, using a cell-free assay, we identified all annotated kinase targets of PIK-75 and subsequently identified CDK1 and CDK2 as targets critical to the ability of PIK-75 to induce apoptosis in glioma.

Using a PI3K $\alpha$ -specific inhibitor in combination with a clinical inhibitor of CDK1 and CDK2, we recapitulated the apoptotic effects of the parental compound, developing a combination therapy that showed reduced toxicity, and that induced apoptosis in vivo in murine xenografts. We then extended these data using clinical inhibitors of Akt and CDKs, providing a preclinical rationale for translating this therapy to patients. Although residual tumors from our in vivo experiments clearly showed apoptosis (increased caspase cleavage compared with monotherapy controls), we did not observe frank regression, an observation that may bear on translational relevance.

Cell cycle deregulation is a hallmark of many cancers, and CDK inhibitors have been developed and screened as anticancer agents. A number of recently developed CDK inhibitors like roscovitine show promise in clinical trials (23). A major challenge in designing such trials is to ensure that a therapeutic response limited to a subset of patients is not overlooked. In this regard, it is clear that the synthetic-lethal approach observed here is most robust in gliomas that are wild type for PTEN, an observation that should be considered, should this combination of agents be moved forward clinically. We also demonstrate that inhibition of Akt could potentiate the apoptotic effect in *PTEN*<sup>MT</sup> glioma cells, suggesting that very high levels of Akt might be abrogating the synthetic-lethal effects in *PTEN*<sup>MT</sup> glioma and breast cancers.

Current clinical trials are testing PI3K and CDK inhibitors with increased specificity and improved drug-like properties, as well as investigating combinatorial interactions with other agents (23, 24). Our data demonstrate that PI3K and CDK1/2 inhibitors act in a synthetic-lethal manner to induce apoptosis in *PTEN*<sup>WT</sup> glioma xenografts in vivo, presenting a clinically translatable therapeutic for patients with glioma with potential for improved outcomes over cytostatic therapies.

## Materials and Methods

**Cell Lines and Reagents.** Human glioma cell lines LN229, U87, U373, 5F767, human glioma GBM43 and GBM14 cells, human breast cancer cell lines BT549, MDAMB231, T47D, and BAX-WT, and BAX-KO MEFs were grown in 10% (vol/vol) FBS. Human breast cancer cell line SUM149 was grown in 5% (vol/vol) FBS. PIK-90, PI-103, and PIK-75 were synthesized as described (7). LY294002 was purchased from Cell Signaling; CDK1 [ $IC_{50}$ : 5.8  $\mu$ M (CDK1/cyclin B); 25  $\mu$ M (CDK5)], CDK2 [ $IC_{50}$ : 6.6, 0.41, 5.5, 15, and 3.9  $\mu$ M for CDK1/cyclin B, CDK2/cyclin A, CDK4/cyclin D, CDK5/p25, and CDK7/cyclin H, respectively], and Akti-1/2 inhibitors were from Calbiochem; and roscovitine was from Sigma (for in vitro experiments) or synthesized by Nathanael Gray (for in vivo experiment). MK-2206 [8-[4-(1-aminocyclobutyl)phenyl]-9-phenyl-1,2,4-triazolo[3,4-f] [1,6]naphthyridin-3(2H)-one hydrochloride] and MK-7965 [(S)-(-)-2-(1-[3-ethyl-7-[(1-oxy-pyridin-3-ylmethyl) amino] pyrazolo[1,5-a]pyrimidin-5-yl]piperidin-2-yl)ethanol] were generously provided by Steven M. Townson and Merck.

**Flow Cytometry.** For cell cycle analysis, nuclei were stained with 5  $\mu$ M propidium iodide containing 125 units/mL RNase and analyzed in a FACScalibur flow cytometer (Becton Dickinson). DNA histograms were modeled offline using Modfit-LT software (Verity Software). Apoptosis was detected by measurement of sub-G<sub>1</sub> fraction or by flow cytometry for annexin V-FITC according to the protocol of the manufacturer (BioVision). *P* values of statistical significance were obtained by Student's *t* test.

**siRNA Transfection and Retroviral Transduction.** For transfections, control siRNA (Santa Cruz Biotechnology) and CDC2 (CDK1) and CDK2 siRNA (Dharmacon) were transfected using Lipofectamine 2000 (Invitrogen) as described previously (25). To generate retrovirus, we cotransfected the packaging cell line HEK 293T with pMSCV-CDK1 and/or pMSCV-CDK2, along with plasmids expressing gag/pol and VSVg (vesicular stomatitis virus glycoprotein), using Effectene transfection reagent (Qiagen). At 48 h posttransfection, the viral supernatants were filtered and used to infect LN229 cells. Infected cells were selected with 0.5  $\mu\text{g}/\text{mL}$  puromycin. The cloning region of human Survivin cDNA was cloned by PCR into the pENTR $\beta$ -TOPO plasmid (Invitrogen) and then subcloned by gateway recombination into pLENTI CMV/TO Puro DEST plasmid [Addgene (26)]. Lentiviral particles were generated in HEK293T cells as described previously (ViraPower protocol; Invitrogen). LN229 cells were transduced and selected for 2 wk with puromycin.

**Immunoblotting.** Membranes were blotted with p-Akt (Ser473), Akt (pan), p-Erk (Thr202/Tyr204), p-S6 ribosomal protein (Ser235/236), S6 ribosomal protein, p-Rb (Ser807/811), cleaved-PARP (Asp214), BAX, CDK1, CDK2, Survivin (all from Cell Signaling), Erk2 (Santa Cruz),  $\beta$ -tubulin, or GAPDH (Millipore). Bound antibodies were detected with HRP-linked anti-mouse or anti-rabbit IgG (Calbiochem), followed by ECL (Amersham). Cells positive for cleaved caspase 3 were detected as described previously (27).

**Immunohistochemistry.** Tumor tissues were fixed in 4% paraformaldehyde (PFA) and 20% sucrose and then embedded in OCT compound as described (28). Sections of 10- $\mu\text{m}$  thickness were cut and placed on silane-coated slide

glasses. Sections were incubated at 4  $^{\circ}\text{C}$  overnight with mouse monoclonal anti-Ki-67 (1:1; Zymed) and rabbit polyclonal anti-cleaved caspase 3 antibody (1:200; Cell Signaling) and at room temperature with anti-mouse Alexa Fluor 488 and anti-rabbit Alexa Fluor 555 secondary antibodies (1:100, Molecular Probes) for 1 h. Nuclei were labeled with Hoechst. Sections were mounted with Vectashield mounting media and analyzed with a Zeiss 510 LSM confocal microscope.

**Xenografts.** Human primary GBM43 cells ( $10^6$ ) were injected s.c. just caudal to the left forelimb in 4- to 6-wk-old female *BALB/c nu/nu* mice (Harlan; Sprague-Dawley). After tumors were established (50–100  $\text{mm}^3$ ), mice were randomly allocated to daily i.p. treatment with 40 mg/kg PIK-90 (DMSO:H<sub>2</sub>O), 50 mg/kg roscovitine (DMSO:PBS), 40 mg/kg PIK-90 plus 50 mg/kg roscovitine, and DMSO:H<sub>2</sub>O:PBS (control). Tumor diameters were measured with calipers at 3-d intervals, and volumes were calculated using the following formula: volume ( $\text{mm}^3$ ) =  $1/2(\text{width}^2 \times \text{length})$ . All mouse experimentation was performed in accordance with protocols approved by the IACUC at the University of California, San Francisco and adhered to the National Institutes of Health *Guide for the Care and Use of Laboratory Animals* (29).

**ACKNOWLEDGMENTS.** This work was supported by grants from the Brain Tumor Society, Accelerate Brain Cancer Cure, the Burroughs Wellcome Fund, the Howard Hughes Medical Institute, the Mount Zion Health Fund, National Institutes of Health (NIH) Specialized Programs of Research Excellence (SPORE) Grant CA097257, NIH Grant 1R01CA136717, the Susan G. Komen Foundation, and the Samuel Waxman Cancer Research Foundation.

- Wong AJ, et al. (1987) Increased expression of the epidermal growth factor receptor gene in malignant gliomas is invariably associated with gene amplification. *Proc Natl Acad Sci USA* 84:6899–6903.
- Humphrey PA, et al. (1988) Amplification and expression of the epidermal growth factor receptor gene in human glioma xenografts. *Cancer Res* 48:2231–2238.
- Cancer Genome Atlas Research Network(2008) Comprehensive genomic characterization defines human glioblastoma genes and core pathways. *Nature* 455:1061–1068.
- Fung AS, Wu L, Tannock IF (2009) Concurrent and sequential administration of chemotherapeutic and the Mammalian target of rapamycin inhibitor temsirolimus in human cancer cells and xenografts. *Clin Cancer Res* 15:5389–5395.
- Fan QW, et al. (2006) A dual PI3 kinase/mTOR inhibitor reveals emergent efficacy in glioma. *Cancer Cell* 9:341–349.
- Fan QW, et al. (2007) A dual phosphoinositide-3-kinase alpha/mTOR inhibitor cooperates with blockade of epidermal growth factor receptor in PTEN-mutant glioma. *Cancer Res* 67:7960–7965.
- Knight ZA, et al. (2006) A pharmacological map of the PI3-K family defines a role for p110alpha in insulin signaling. *Cell* 125:733–747.
- Hayakawa M, et al. (2007) Synthesis and biological evaluation of sulfonylhydrazonesubstituted imidazo[1,2-a]pyridines as novel PI3 kinase p110alpha inhibitors. *Bioorg Med Chem* 15:5837–5844.
- Hayakawa M, et al. (2007) Synthesis and biological evaluation of imidazo[1,2-a]pyridine derivatives as novel PI3 kinase p110alpha inhibitors. *Bioorg Med Chem* 15:403–412.
- Schmid AC, Byrne RD, Vilar R, Woscholski R (2004) Bisperoxovanadium compounds are potent PTEN inhibitors. *FEBS Lett* 566:35–38.
- Mirza AM, Kohn AD, Roth RA, McMahon M (2000) Oncogenic transformation of cells by a conditionally active form of the protein kinase Akt/PKB. *Cell Growth Differ* 11:279–292.
- Wei MC, et al. (2001) Proapoptotic BAX and BAK: A requisite gateway to mitochondrial dysfunction and death. *Science* 292:727–730.
- Lindsten T, et al. (2000) The combined functions of proapoptotic Bcl-2 family members bak and bax are essential for normal development of multiple tissues. *Mol Cell* 6:1389–1399.
- Hu B, Mitra J, van den Heuvel S, Enders GH (2001) S and G2 phase roles for Cdk2 revealed by inducible expression of a dominant-negative mutant in human cells. *Mol Cell Biol* 21:2755–2766.
- Malumbres M, Barbacid M (2009) Cell cycle, CDKs and cancer: A changing paradigm. *Nat Rev Cancer* 9:153–166.
- Benson C, et al. (2007) A phase I trial of the selective oral cyclin-dependent kinase inhibitor seliciclib (CYC202; R-Roscovitine), administered twice daily for 7 days every 21 days. *Br J Cancer* 96:29–37.
- Hsieh WS, et al. (2009) Pharmacodynamic effects of seliciclib, an orally administered cell cycle modulator, in undifferentiated nasopharyngeal cancer. *Clin Cancer Res* 15:1435–1442.
- Hui AB, et al. (2009) Therapeutic efficacy of seliciclib in combination with ionizing radiation for human nasopharyngeal carcinoma. *Clin Cancer Res* 15:3716–3724.
- Sarkaria JN, et al. (2006) Use of an orthotopic xenograft model for assessing the effect of epidermal growth factor receptor amplification on glioblastoma radiation response. *Clin Cancer Res* 12:2264–2271.
- Kim EH, Kim SU, Shin DY, Choi KS (2004) Roscovitine sensitizes glioma cells to TRAIL-mediated apoptosis by downregulation of survivin and XIAP. *Oncogene* 23:446–456.
- Hirai H, et al. (2010) MK-2206, an allosteric Akt inhibitor, enhances antitumor efficacy by standard chemotherapeutic agents or molecular targeted drugs in vitro and in vivo. *Mol Cancer Ther* 9:1956–1967.
- Parry D, et al. (2010) Dinaciclib (SCH 727965), a novel and potent cyclin-dependent kinase inhibitor. *Mol Cancer Ther* 9:2344–2353.
- Lapenna S, Giordano A (2009) Cell cycle kinases as therapeutic targets for cancer. *Nat Rev Drug Discov* 8:547–566.
- Maira SM, et al. (2008) Identification and characterization of NVP-BE2253, a new orally available dual phosphatidylinositol 3-kinase/mammalian target of rapamycin inhibitor with potent in vivo antitumor activity. *Mol Cancer Ther* 7(7):1851–1863.
- Fan QW, Weiss WA (2005) RNA interference against a glioma-derived allele of EGFR induces blockade at G2M. *Oncogene* 24:829–837.
- Campeau E, et al. (2009) A versatile viral system for expression and depletion of proteins in mammalian cells. *PLoS ONE* 4:e6529.
- Fan QW, et al. (2010) Akt and autophagy cooperate to promote survival of drug-resistant glioma. *Sci Signal* 3:ra81.
- Fan QW, et al. (2003) Combinatorial efficacy achieved through two-point blockade within a signaling pathway—a chemical genetic approach. *Cancer Res* 63:8930–8938.
- Committee on Care and Use of Laboratory Animals (1985) *Guide for the Care and Use of Laboratory Animals* (Natl Inst Health, Bethesda), DHHS Publ No (NIH) 85–23.